Observation of the Fano-Kondo Antiresonance in a Quantum Wire with a Side-Coupled Quantum Dot

Masahiro Sato, Hisashi Aikawa, Kensuke Kobayashi, Shingo Katsumoto, and Yasuhiro Iye
Institute for Solid State Physics, University of Tokyo, 5-1-5 Kashiwanoha, Chiba 277-8581, Japan
(Received 4 October 2004; published 1 August 2005)

We have observed the Fano-Kondo antiresonance in a quantum wire with a side-coupled quantum dot. In a weak coupling regime, dips due to the Fano effect appeared. As the coupling strength increased, conductance in the regions between the dips decreased alternately. From the temperature dependence and the response to the magnetic field, we conclude that the conductance reduction is due to the Fano-Kondo antiresonance. At a Kondo valley with the Fano parameter $q \approx 0$, the phase shift is locked to $\pi/2$ against the gate voltage when the system is close to the unitary limit in agreement with theoretical predictions by Gerland *et al.* [Phys. Rev. Lett. **84**, 3710 (2000)].

DOI: 10.1103/PhysRevLett.95.066801 PACS numbers: 73.21.La, 72.15.Qm, 73.23.Hk

The experimental realization of the Kondo effect [1] in a semiconductor quantum dot (QD) has opened up a new human-made stage to investigate many body effects [2]. In a previous paper, we have shown that spin scattering at a QD, which means the creation of a spin-entangled state between a localized spin and a conduction electron, leads to quantum decoherence [3,4]. At the same time, however, such an entangled state is a starting point to build a Kondo singlet [5], in which the coherence of electrons is expected to be recovered.

The direct evidence for the coherence of the Kondo state is the interference effect through a QD in the Kondo state. Ji *et al.* measured the phase shift of electrons through a dot in the Kondo state in an Aharonov-Bohm (AB) ring [6], and found that the phase shift significantly varies even on the Kondo plateau of conductance, which may suggest the breakdown of the Anderson model. However, the difficulty in measuring the phase shift in AB geometry is pointed out [7], and experiments in simpler structures such as a stub resonator [a schematic diagram is shown in Fig. 1(a)] [8,9] are desired.

Some of the present authors have reported the observation of the Fano antiresonance in a quantum wire with a side-coupled QD [10], which is a kind of a stub resonator. The Fano effect [11] is a consequence of interference between a localized state and a continuum, which correspond to a state in the QD and that in the wire, respectively. It appears as a characteristic line shape in the conductance G as

$$G(\epsilon) \propto (\epsilon + q)^2/(\epsilon^2 + 1), \quad (1)$$

where ϵ is the energy difference from the resonance position normalized with the width of the resonance, and q is Fano's asymmetric parameter [12]. The Fano parameter represents the degree of distortion and $q = 0$ corresponds to an antiresonance dip. The Fano-Kondo effect—the Fano effect that appears in the Kondo cloud—is hence sensitive to coherence and phase shifts [13]. In this Letter, we report the observation of the Fano-Kondo antiresonance in a quantum wire with a side-coupled QD. Phase shift locking to $\pi/2$ is deduced from the analysis of the line shape of the antiresonance.

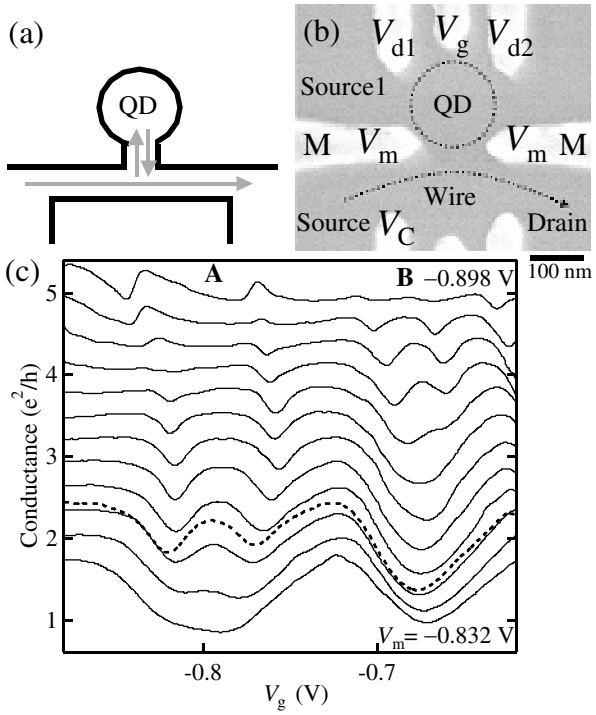

FIG. 1. (a) Schematic diagram of a stub resonator. (b) Scanning electron micrograph of the device. The white areas are metallic gates made of Au/Ti. The dot and the wire are indicated by dotted lines. Conduction between Source1 and Drain is used to measure the direct transport through the dot, while that between Source and Drain gives the main results of this Letter. (c) Conductance of the wire measured at several coupling strengths tuned by V_m. The base temperature is 30 mK. The step in V_m is 6 mV, and the data are offset by $0.3e^2/h$ for clarity. The broken line shows the data at $V_m = -0.846$ V shown in Fig. 2.

Our device consists of a quantum dot and a quantum wire defined in a two-dimensional electron gas (2DEG, sheet carrier density 3.8×10^{15} m^{-2}, mobility 80 m^2/Vs) formed at a GaAs/Al_xGa_{1-x}As heterostructure. Au/Ti metallic gates were deposited as shown in Fig. 1(b). A QD is defined by the upper three gates and the two gates marked as ''M'' (M gates). The lower three gates adjust the conductance of the wire. The middle of the upper gates is used to control the potential of the dot (gate voltage V_g) and M gates tune the coupling between the dot and the wire (gate voltage V_m). It was confirmed that the system works as a quantum wire with no quantum dot when M gates are pinched off. Tuning the coupling strength by M gates induces the electrostatic potential shift of the dot, whereas the potential shift by V_g causes little change in the coupling strength. Accordingly, the potential shift by V_m can be compensated by V_g (approximately $\Delta V_g = -4.5\Delta V_m$ in the present sample). For the sake of a simpler description, we henceforth redefine $V_g \equiv V_g(\text{raw}) - 4.5(V_m + 0.846)$. In order to attain a large value of Kondo temperature T_K, the device was designed to make the dot size smaller than that used in Ref. [10]. The dot is placed close to the wire to avoid temperature dependence associated with a change of the coherence length, which is unfavorable for the present study. Although the proximity of the dot to the wire would cause a Fano-charging mixing effect [14], it is less severe in a comparatively strong coupling regime explored here. The sample was cooled in a dilution refrigerator down to 30 mK and was measured by standard lock-in techniques in a two-terminal setup.

In order to obtain the relevant parameters of the dot, we first measured the direct charge transport through the dot (from ''Source1'' to ''Drain'' in Fig. 1(b)] by slightly opening V_{d1} and by closing V_{d2} and V_c. The average level spacing Δ obtained from excitation spectroscopy is about 0.3 meV, which gives the dot diameter as about 170 nm and the total number of electrons as about 90. The electron temperature estimated from the widths of resonance peaks followed the fridge temperature down to 100 mK, and severe saturation occurred below that. Then the direct connection was pinched off by V_{d1} and the wire was opened by V_c. The wire conductance far from (anti)resonances was adjusted to be about $G_q \equiv 2e^2/h$, i.e., at the first step of the conductance staircase.

Figure 1(c) shows the wire conductance against V_g at various coupling strengths adjusted by V_m. In a weak coupling regime [at the top of Fig. 1(c)], Coulomb ''dips'' appear, reproducing the previous result [10]. This is due to the destructive interference, i.e., the Fano antiresonance. These dips are regularly placed, and the averaged period is the same as that of the Coulomb oscillation in the direct transport. This indicates that the dips originate from the QD. As the coupling strength increases, conductance between the dips (Coulomb valleys) decreases alternately. These reductions connect two neighboring dips into one (in regions A and B). We have observed four such valleys (as shown in Fig. 2) where the conductance decreases as the coupling strength increases. We next confirm that these reductions are due to the Fano-Kondo antiresonance, then discuss the obtained information.

The upper panel of Fig. 2 shows the zero-bias wire conductance as a function of V_g at three different temperatures for a medium coupling strength. The closed bars indicate the positions of the Coulomb dips. For valley B, the positions cannot be resolved directly and are extrapolated from the positions at $V_m = -0.886$ V. In the four regions indicated as A–D, conductance decreases with decreasing temperature. The Kondo effect for spin 1/2 emerges for a QD with an odd number of electrons. Hence, it usually appears alternately at Coulomb valleys as we observed at Kondo valleys A–D.

The distances between the Coulomb dips are shorter at the Kondo valleys than those at the neighboring valleys. The level spacing Δ obtained from this difference of the distances is in good agreement with Δ obtained from excitation spectroscopy. This means the simple ''spin-pair'' picture is held and the conditions for the Kondo effect are fulfilled at valleys A–D.

The lower panel of Fig. 2 is a color scale plot of the conductance on the plane of V_g and the source-drain bias voltage V_{sd}. The conductance drops about $V_{sd} = 0$ mV at the Kondo valleys. Note that V_{sd} is not directly applied to the dot but to the wire. The wire by itself can show nonlinear conductance [15]. In this experiment, however, the nonlinearity of the wire is small, because the wire is under the plateau condition and the scale of V_{sd} is magnitudes smaller than that in the previous papers [15]. Furthermore,

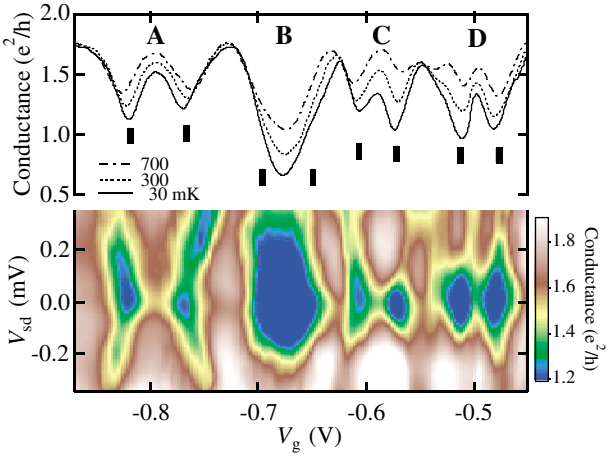

FIG. 2 (color). Upper: Zero-bias conductance of the quantum wire at three different temperatures as a function of the gate voltage V_g at $V_m = -0.846$ V. The bars indicate the positions of Coulomb dips and A–D indicate the Coulomb valleys where the Kondo effect emerges. Lower: Color scale plot of the conductance on the V_g-V_{sd} plane at 30 mK. Both the upper and the lower panels use the same V_g axis.

the response to V_g and the reversed Coulomb diamond-like structure (not well resolved in Fig. 2) indicate that the zero-bias dips originate from the Kondo effect of the dot. The charging energy U estimated from the reversed Coulomb diamond ranges from 0.3 to 0.5 meV. For a quantitative comparison with existing theories, we should be careful to multilevel effect, which is usually ignored by taking the limit of infinite Δ (or charging energy). Such ''single-level'' approximation is expected to hold when the separation of Coulomb peaks (dips) is clear. We therefore concentrate on dip A, which shows the clearest separation.

The upper panel of Fig. 3(a) shows detailed temperature dependence of $G(V_g)$ at Kondo valley A. We obtained the Kondo temperature T_K from the form [16]

$$G(T) = G_0 - G_1[T_K'^2/(T^2 + T_K'^2)]^s, \quad (2)$$

where G_1, $T_K' \equiv T_K/\sqrt{2^{1/s} - 1}$, and s are fitting parameters. G_0 was fixed to $1.8e^2/h$, the wire conductance far from the antiresonance. Examples of the fitting are shown in Fig. 3(b). The data below 120 mK are not taken into the fitting, considering the electron temperature saturation. From the fitting, $s = 0.25 \pm 0.04$ was obtained, which is in accordance with the prediction for spin 1/2 impurities. The obtained T_K are plotted against V_g in the lower panel of Fig. 3(a). T_K depends parabolically on V_g with the bottom around the midpoint of the Kondo valley just like the previous reports [17]. This dependence agrees well with $T_K = \sqrt{\Gamma U}\exp[\pi\epsilon(\epsilon + U)/\Gamma U]/2$, where Γ is the dot-wire coupling and ϵ is the single electron level measured from the Fermi level. We obtained $U = 0.39 \pm 0.03$ meV and $\Gamma = 0.30 \pm 0.02$ meV by fitting the above function to T_K.

Figure 4(a) shows the splitting of the zero-bias conductance dip under the external magnetic field parallel to the 2DEG. The splitting is proportional to the field as shown in Fig. 4(b) and attributed to the Zeeman splitting of the Kondo anomaly. From the slope of the fitted line, we obtain the g factor of electrons as $|g| = 0.33$, which is close to that reported for GaAs/Al_xGa_{1-x}As 2DEG [18].

So far we have confirmed that the conductance reduction in regions A–D in Fig. 2 is due to the Fano-Kondo antiresonance. In the side-coupled geometry, only destructive interference can cause the conductance reduction. The observation of the Kondo effect through the pure interference effect manifests that electron transport through the Kondo cloud is coherent as predicted [8].

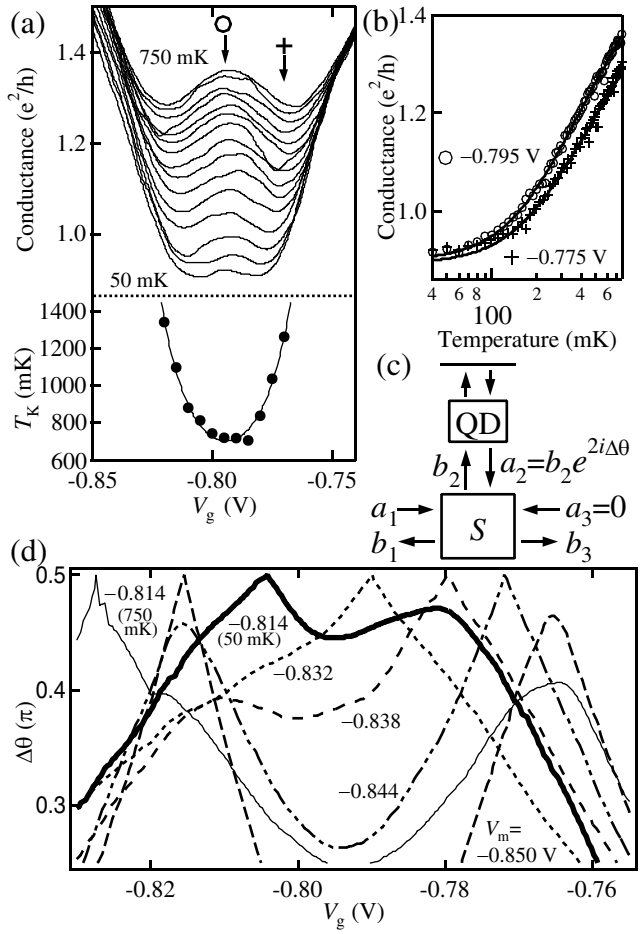

FIG. 3. (a) Upper: Conductance at temperatures from 750 to 50 mK with the step of 50 mK at $V_m = -0.814$ V. Lower: Kondo temperatures T_K obtained from the temperature dependence. (b) Examples of the fitting to obtain T_K. The gate voltages adopted here are indicated by arrows in (a). (c) Schematic diagram of a simple quantum circuit model of the system. The factor 2 of $\Delta\theta$ in a_2 is due to the reflection. (d) Phase shift of the QD obtained for the data in (a) at $V_m = -0.814$ V and 50 mK (thick line), 750 mK (thin line), and for the data in Fig. 1(c) at $V_m = -0.832$, -0.838, -0.844, and -0.850 V (dotted lines), based on the model shown in (c). The data folding at $\pi/2$ is due to taking plus of the double sign in (4).

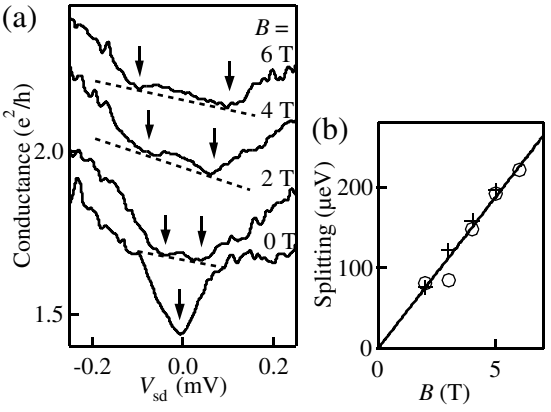

FIG. 4. (a) Conductance versus V_{sd} at Kondo valley A under various magnetic fields up to 6 T. The arrows indicate the positions of the conductance dips, which are determined by fitting two Gaussian curves. The broken lines are eye guides to show the baselines. (b) Distance between two dip positions versus the magnetic field. The data were taken at Kondo valleys A (open circles) and C (crosses) in Fig. 2. The line corresponds to $|g| = 0.33$.

In Fig. 1(c), two dips merge into one in regions A and B. This means the system almost reaches the unitary limit [17]. This is consistent with the obtained T_K shown in the lower panel of Fig. 3. The residual conductance at the "unitary limit" Kondo valleys (e.g., $0.7e^2/h$ at valley B in Fig. 2) is probably due to the finite area between the wire and the dot, which works as a resonator and spoils the perfect reflection [9], while the phase shift is unchanged because $q \approx 0$.

When the coupling is weak [at the top of Fig. 1(c)], the two dips at both sides of valley A have asymmetric Fano line shapes ($q \neq 0$). It has been anticipated that symmetry of transport through a QD is dominated by a few states with an anomalously strong coupling to an electrode (strong coupling states, SCSs) [19]. In a weak coupling regime, the q's of the two dips at both sides of valley A are hence determined by an SCS. As the coupling strength increases, however, the values of q approach zero, indicating that the coupling strength is renormalized and the Kondo state takes over the SCS.

We now discuss the phase shift of the Kondo state, which can be obtained from the analysis along the scattering form of conductance. A simple model of the system: A three branch S matrix and a reflector (the QD) are shown in Fig. 3(d). Here we take the S matrix simply as

$$\begin{pmatrix} b_1 \\ b_2 \\ b_3 \end{pmatrix} = \begin{pmatrix} 0 & 1/\sqrt{2} & 1/\sqrt{2} \\ 1/\sqrt{2} & -1/2 & 1/2 \\ 1/\sqrt{2} & 1/2 & -1/2 \end{pmatrix} \begin{pmatrix} a_1 \\ a_2 \\ a_3 \end{pmatrix}. \quad (3)$$

Assuming the absence of reflection from the electrodes, we put $a_3 = 0$. And taking the QD as a transmitter plus a perfect reflector, we put $a_2 = b_2 \exp(2i\Delta\theta)$ and $a_1 = 1$ for unitary input. Then the phase shift $\Delta\theta$ is easily obtained as

$$\Delta\theta = \arg\left(\frac{\sqrt{2} - 2b_3}{b_3 - \sqrt{2}}\right), \qquad \arg(b_3) = \pm\cos^{-1}\left(\frac{3|b_3|}{2\sqrt{2}}\right). \quad (4)$$

Here b_3 is the complex transmittance and is related with the conductance through the Landauer formula as $G = G_0'(\text{constant}) + (e^2/h)|b_3|^2$. The specific form of (3) does not spoil the generality. The time-reversal symmetry, the unitarity, and $q = 0$ impose strong constraints on the S matrix, and the residual freedom has very little effect.

Figure 3(d) thus shows calculated $\Delta\theta(V_g)$. Here we take plus of the double sign in (4), which causes the virtual folding at $\pi/2$. This is due to the special condition of $q = 0$, and the folding does not disturb the confirmation of locking to $\pi/2$. As temperature decreases from 750 to 50 mK and the coupling becomes stronger from $V_m = -0.850$ to -0.814 V, the phase shift variation approaches the stationary line of $\pi/2$ at the Kondo valley. This is in accordance with the existing theories [20] and in contrast to the previous result [6], where only locking to π at the pre-Kondo region was observed. The difference may come from the width of the energy levels [20] or from the geometry of the interferometer, though we have no conclusive opinion at present.

In Fig. 2, zero-bias anomalies appear while no voltage was directly applied to the dot. This indicates that the Kondo cloud spreads into the wire and is affected by V_{sd}. This is reasonable considering the size of the Kondo cloud $\hbar v_F/k_B T_K$ (v_F: Fermi velocity), which exceeds 2 μm for T_K less than 1 K [21]. The present structure provides the means to investigate the size of the Kondo cloud.

In summary, we have observed the Fano-Kondo antiresonance in a quantum wire with a side-coupled dot. Phase shift locking to $\pi/2$ is deduced from the line shape of the antiresonance.

This work is supported by a Grant-in-Aid for Scientific Research and by a Grant-in-Aid for COE Research from the Ministry of Education, Culture, Sports, Science, and Technology of Japan.

[1] J. Kondo, in *Solid State Physics* (Academic Press, New York, 1969), Vol. 23, p. 13.
[2] D. Goldhaber-Gordon *et al.*, Nature (London) **391**, 156 (1998); S. M. Cronenwett *et al.*, Science **281**, 540 (1998); J. Schmid *et al.*, Physica (Amsterdam) **256B–258B**, 182 (1998).
[3] H. Aikawa *et al.*, Phys. Rev. Lett. **92**, 176802 (2004).
[4] J. König and Y. Gefen, Phys. Rev. Lett. **86**, 3855 (2001); Phys. Rev. B **65**, 045316 (2002).
[5] K. Yosida and A. Yoshimori, *Magnetism V*, edited by H. Suhl (Academic Press, New York, 1973).
[6] Y. Ji *et al.*, Science **290**, 779 (2000); Y. Ji, M. Heiblum, and H. Shtrikman, Phys. Rev. Lett. **88**, 076601 (2002).
[7] A. Aharony *et al.*, Phys. Rev. B **66**, 115311 (2002).
[8] K. Kang *et al.*, Phys. Rev. B **63**, 113304 (2001); A. A. Aligia and C. R. Proetto, Phys. Rev. B **65**, 165305 (2002); M. E. Torio *et al.*, Phys. Rev. B **65**, 085302 (2002).
[9] W. B. Thimm, J. Kroha, and J. von Delft, Phys. Rev. Lett. **82**, 2143 (1999).
[10] K. Kobayashi *et al.*, Phys. Rev. B **70**, 035319 (2004).
[11] U. Fano, Phys. Rev. **124**, 1866 (1961).
[12] K. Kobayashi *et al.*, Phys. Rev. Lett. **88**, 256806 (2002); Phys. Rev. B **68**, 235304 (2003).
[13] W. Hofstetter, J. König, and H. Schöller, Phys. Rev. Lett. **87**, 156803 (2001).
[14] A. C. Johnson *et al.*, Phys. Rev. Lett. **93**, 106803 (2004).
[15] A. Kristensen *et al.*, Phys. Rev. B **62**, 10 950 (2000).
[16] T. A. Costi, A. C. Hewson, and V. Zlatic, J. Phys. Condens. Matter **6**, 2519 (1994); D. Goldhaber-Gordon *et al.*, Phys. Rev. Lett. **81**, 5225 (1998).
[17] W. G. van der Wiel *et al.*, Science **289**, 2105 (2000).
[18] H. W. Jiang and E. Yablonovitch, Phys. Rev. B **64**, 041307(R) (2001).
[19] T. Nakanishi, K. Terakura, and T. Ando, Phys. Rev. B **69**, 115307 (2004).
[20] U. Gerland *et al.*, Phys. Rev. Lett. **84**, 3710 (2000).
[21] P. Simon and I. Affleck, Phys. Rev. B **68**, 115304 (2003).